Journal of the Korean Astronomical Society
51: 5 ∼ 16, 2018 February

http://dx.doi.org/10.5303/JKAS.2018.51.1.5
pISSN: 1225-4614 · eISSN: 2288-890X
http://jkas.kas.org

Escape of Resonantly Scattered Lyβ and Hα from Hot and Optically Thick Media

Seok-Jun Chang[1], Hee-Won Lee[1], Sang-Hyeon Ahn[2], Hogyu Lee[2], Rodolfo Angeloni[3,4], Tali Palma[5], and Francesco Di Mille[6]

[1]Department of Physics and Astronomy, Sejong University, Neungdong-ro 209, Seoul 05006, Korea; hwlee@sejong.ac.kr
[2]Korea Astronomy and Space Science Institute, 776 Daedukdae-ro, Yuseong-gu, Daejeon 34055, Korea
[3]Departamento de Fisica y Astronomia, Universidad de La Serena, Av. J. Cisternas 1200 Norte, La Serena, Chile
[4]Instituto de Investigación Multidisciplinar en Ciencia y Tecnología, Universidad de La Serena, Av. R. Bitrán 1305, La Serena, Chile
[5] Observatorio Astronómico, Universidad Nacional de Córdoba, Laprida 854, Córdoba, Argentina
[6]Las Campanas Observatory, Carnegie Observatories, Casilla 601, La Serena, Chile

Received December 3, 2017; accepted January 19, 2018

Abstract: We investigate the escape of Lyβ from emission nebulae with a significant population of excited hydrogen atoms in the level $n = 2$, rendering them optically thick in Hα. The transfer of Lyβ line photons in these optically thick regions is complicated by the presence of another scattering channel leading to re-emission of Hα, alternating their identities between Lyβ and Hα. In this work, we develop a Monte Carlo code to simulate the transfer of Lyβ line photons incorporating the scattering channel into Hα. Both Hα and Lyβ lines are formed through diffusion in frequency space, where a line photon enters the wing regime after a fairly large number of resonance scatterings with hydrogen atoms. Various line profiles of Hα and Lyβ emergent from our model nebulae are presented. It is argued that the electron temperature is a critical parameter which controls the flux ratio of emergent Lyβ and Hα. Specifically for $T = 3 \times 10^4$ K and Hα line center optical depth $\tau_\alpha = 10$, the number flux ratio of emergent Lyβ and Hα is ~ 49 percent, which is quite significant. We propose that the leaking Lyβ can be an interesting source for the formation of Hα wings observed in many symbiotic stars and active galactic nuclei. Similar broad Hα wings are also expected in Lyα emitting halos found in the early universe, which can be potentially probed by the *James Webb Telescope* in the future.

Key words: radiative transfer — scattering — line: formation — line: profiles

1. Introduction

Hα is one of the strongest optical emission lines in emission nebulae found in a variety of celestial objects including star forming regions, planetary nebulae and supernova remnants. In particular, emission nebulae in symbiotic stars and active galactic nuclei (hereafter AGN) are proposed to be formed through photoionization from a strong far UV source. Symbiotic stars are believed to be binary systems of a white dwarf and a mass losing giant (e.g., Kenyon 1986). The white dwarf component in symbiotic stars exhibits various activities including erratic variability and X-ray emission (e.g., Nuñez et al. 2016), which is attributed to accretion by gravitational capture of a fraction of material lost by the giant companion. AGN are powered by a supermassive black hole with an accretion disk (e.g., Netzer 2015). Strong emission of Hα is also present in Lyα emitting objects in the early universe (Dijkstra 2014).

Spectroscopy using *International Ultraviolet Explorer (IUE)* and *Far Ultraviolet Spectroscopic Explorer (FUSE)* shows that symbiotic stars and AGN also share prominent emission lines with a large range of ionization potentials including O VI and Mg II (e.g., Godon et al. 2012; Sion et al. 2017). High ionization lines are mainly formed in a shallow region on the side illuminated by the strong photoionizing source, whereas low ionization lines are formed in a deep region shielded from highly ionizing radiation. Therefore, the co-existence of high and low ionization lines implies that the emission regions are highly optically thick. Lyα emitters in the early universe exhibit quite extended Lyα halo with significant polarization, which is consistent with considerable scattering optical depth of Lyα (Yang et al. 2011). One consequence of the presence of highly optically thick media is the anomalous flux ratios of Balmer lines, which deviates from those expected from the case B recombination theory.

When the $n = 2$ population of hydrogen is significant, the transfer of Hα line photons can be complicated due to another de-excitation channel. That is, an excited hydrogen atom may de-excite into the ground state, reemitting a Lyβ photon. The alternation of their identity between Hα and Lyβ requires one to treat the transfer of Hα and Lyβ together. In the case where the level $n = 2$ population is negligible compared to the ground state population, Lyβ photons are selectively prevented from escaping the region. The case B recombination theory is well established based on this

Corresponding author: H.-W. Lee

situation, in which Lyman photons are optically thick so that higher Lyman series photons are absorbed by hydrogen atoms to reappear as Balmer or higher series photons.

The typical electron temperature of most emission nebulae is 10^4 K due to balance between heating through ionization and cooling by line emission. However, the thermal properties of emission nebulae in many symbiotic stars are consistent with electron temperature T_e in the range of $10^4 - 4 \times 10^4$ K (e.g., Skopal 2005). In particular, Sekeras & Skopal (2012) reported that broad wings around O VI $\lambda\lambda$1032 and 1038 are consistent with the presence of Thomson scattering media with $T_e \sim 3 \times 10^4$ K in symbiotic stars. Far UV observations of symbiotic stars show very strong resonance doublets O VI $\lambda\lambda$1032, 1038, N V $\lambda\lambda$1238, 1243, and C IV $\lambda\lambda$1548, 1551, which are important coolants of astrophysical plasma with temperature $T \sim 10^5$ K (e.g., Gnat & Sternberg 2007). O VI lines are very strong in symbiotic stars and quasars, implying that Hα emission may also be contributed in a significantly hot environment of $T \sim 10^5$ K.

With this temperature, the number of hydrogen atoms in an excited state with $n = 2$ is non-negligible compared to that in the ground state $n = 1$. In a medium that is optically thick at line center, a resonance line photon escapes through diffusion in frequency space after a large number of local scatterings. Due to the high optical depth for a photon with wavelength near line center, it can escape only if it is occasionally scattered off an atom with a large thermal motion along the final line of sight. This last scattering allows the photon to enter the wing regime, in which the medium is optically thin. This also implies that the emergent resonance line profile will exhibit a double-peak structure or equivalently will be characterized by the presence of a central dip (e.g., Neufeld 1990; Gronke et al. 2016).

In the radiative transfer of optically thick Hα-Lyβ, diffusion in frequency space is also essential in a more complicated way. The probability of making a de-excitation into $1s$ state is about 7 times higher than into $2s$ state, so that we may expect that diffusion of Lyβ is more significant than Hα in the Doppler factor space. A Monte Carlo technique provides a straightforward method to treat the transfer of resonance line photons, as is shown by many researchers. In this paper, we develop a Monte Carlo code to deal with the radiative transfer of Hα-Lyβ in optically thick media.

2. MONTE CARLO APPROACH TO RADIATIVE TRANSFER

2.1. Atomic Physics

If an emission nebula is moderately optically thick at Hα line center, the transfer of Hα photons mimics that of typical resonance line photons in that escape is made through diffusion in frequency space (e.g., Osterbrock 1962). In this respect, description of the transfer of Hα in an optically thick medium may start with the case of resonance line photons. Adams (1972) presented his early investigation of resonance line radiative transfer using "Feautrier's method" to show that the mean number of scatterings is almost proportional to the line center optical depth of the medium. Diffusive nature in frequency space of the radiative transfer of resonantly scattered photons in optically thick media is beautifully illustrated in an analytical way by Neufeld (1990).

The resonance line radiative transfer is also studied efficiently by adopting a Monte Carlo technique. In particular, the transfer of Lyα is very important to understand the physical properties of the intergalactic medium and star formation history in the early universe (e.g., Dijkstra 2014; Ouchi et al. 2010; Yang et al. 2011). A Monte Carlo approach turns out to be an efficient method to compute the profile and polarization of resonantly scattered Lyα (e.g., Ahn et al. 2003; Ahn & Lee 2015).

A typical emission nebula around the hot white dwarf of symbiotic stars has a physical dimension of $R \sim 10^{13}$ cm and a proton number density of $n_p \sim 10^8$ cm^{-3}. A neutral fraction of 10^{-4} implies that H I column density may reach $N_{HI} \sim 10^{17}$ cm^{-2}, which is consistent with proposal that the emission nebula is ionization bounded. Assuming as Boltzmann distribution with a temperature T, the Lyβ line center optical depth is given by

$$\tau_\beta = N_{HI,1s}\sigma_{\nu_0} \tag{1}$$

where $N_{HI,1s}$ is the column density of neutral hydrogen in the ground state and σ_{ν_0} is the total cross section at Lyβ line center. For a typical resonance line with a Gaussian line profile, the line center cross section is of order $10^{-13}T_4^{-1/2}$ cm^2, where $T_4 = T/10^4$ K is the temperature in units of 10^4 K (e.g., Rybicki & Lightman 1985).

The branching ratios of the two channels are obtained by considering the spontaneous transition rates into $1s$ and $2s$ states from $3p$ state. Following Sakurai (1967) the spontaneous transition rate from state A to state B is

$$w_{BA} = \left(\frac{e^2}{4\pi\hbar c}\right)\frac{4}{3}\frac{\omega_{BA}^3}{c^2}|x_{BA}|^2, \tag{2}$$

where ω_{BA} and $|x_{BA}|$ are the angular frequency and matrix element of the position operator between the states A and B. The matrix elements are

$$\begin{aligned} |x_{1s,np}| &= \left[\frac{2^8 n^7 (n-1)^{2n-5}}{3(n+1)^{2n+5}}\right]^{1/2} a_B \\ |x_{2s,np}| &= \left[\frac{2^{17} n^7 (n^2-1)(n-2)^{2n-6}}{3(n+2)^{2n+6}}\right]^{1/2} a_B \end{aligned} \tag{3}$$

where $a_B = \hbar^2/m_e e^2$ is the Bohr radius (e.g., Saslow & Mills 1969).

From Equation (2) we obtain the ratio of transition probabilities from $3p$ to $2s$ and $1s$

$$\frac{w_{3p\to 2s}}{w_{3p\to 1s}} = \frac{\omega_{23}^3}{\omega_{13}^3}\frac{|x_{2s,3p}|^2}{|x_{1s,3p}|^2} = \left(\frac{4}{5}\right)^9 \simeq 0.1342. \tag{4}$$

Another way to look at this relation in terms of the oscillator strengths $f_{1s,3p}$ and $f_{2s,3p}$ is

$$\frac{w_{3p\to 2s}}{w_{3p\to 1s}} = \frac{\omega_{23} f_{2s,3p}}{\omega_{13} f_{1s,3p}} = \left(\frac{4}{5}\right)^9 \tag{5}$$

where the numerical values of the oscillator strengths are $f_{1s,3p} = 0.07910, \quad f_{2s,3p} = 0.4349$ (e.g., Rybicki & Lightman 1985). This implies that out of 8 scattering events about one transition is made into the $2s$ state with an emission of Hα (e.g., Chang et al. 2015; Lee 2013).

The line center optical depth τ_α of Hα due to hydrogen atoms in the $2s$ state is then related to τ_β by

$$\tau_\alpha = 4e^{-\Delta E/kT}\tau_\beta, \tag{6}$$

where k is the Boltzmann constant and $\Delta E = 10.2$ eV is the energy difference between the hydrogen $1s$ and $2s$ states. For $T = 3\times 10^4$ K, the ratio $\tau_\alpha/\tau_\beta \simeq 0.0663$. In this work, the physical radius of a spherical emission nebula is measured by the line center optical depth.

Hα line photons also arise from $3s-2p$ and $3d-3p$ transitions. These $3s-2p$ and $3d-2p$ transitions are meaningful only for initial generation of an H α photon that may directly escape. This is because if it is absorbed by another hydrogen atom in the $2p$ state, then effectively there is no generation of an $H\alpha$ photon from $3s-2p$ and/or $3d-2p$ transitions. If it is scattered by a hydrogen atom in the $2s$ state, then it is an identical process as we inject an Hα photon generated from $3p-2s$ transition. In an optically thick medium, directly escaping fraction will be limited to those generated near the surface, which may be negligible and disregarded in this work

2.2. Monte Carlo Approach

Ahn & Lee (2015) provided a detailed description of their Monte Carlo code, which is also used in this work. Figure 1 illustrates the mechanism of radiative transfer of Hα and Lyβ in an emission nebula. The $1s$ population being larger than $2s$ that of, implies that the line center optical depth Lyβ of is larger than that of Hα, requiring higher scattering numbers for Lyβ to escape from the nebula. Because the branching into Lyβ is about 7 times more probable than that into Hα, on average a typical Lyβ photon suffers 8 scatterings locally before it changes its identity into Hα.

In this work, Hα line photons are generated uniformly in a sphere with the line center optical depth τ_α ranging from 1 to 100. A schematic description of our code is as follows. The simulation starts with a generation of an initial Hα photon at a random position $\mathbf{r}$ in the sphere characterized by τ_α and τ_β. The initial wavevector $\hat{\mathbf{k}}$ of propagation is chosen from an isotropic distribution, and a Gaussian random deviate is used to assign the initial Doppler factor v along its direction of propagation.

A uniform random number X between 0 and 1 is generated to determine the optical depth τ the photon is supposed to traverse by the relation

$$\tau = -\ln(1-X). \tag{7}$$

This optical depth is converted to physical free path length s by the relation

$$\frac{s}{R} = \frac{\tau}{\tau_\alpha}\exp\left(\frac{v^2}{v_{th}^2}\right), \tag{8}$$

where R is the radius of the spherical emission region. Here, $v_{th} = \sqrt{2kT/m_H}$ is the thermal speed of hydrogen, whose mass is m_H. If the free path ends up inside the sphere, then a new scattering site is generated where we choose the wavevector of a scattered photon.

In the frame of the scattering atom, the incident and outgoing photons are line center photons in the case of resonance scattering. Therefore, the velocity component v_1 along the incident wavevector of the emitting atom coincides with that of the receiving atom. In a Monte Carlo approach, one needs to specify the Doppler factor of a new scattered photon along its propagation direction given the Doppler factor along the incident direction. Defining the scattering plane spanned by the incident and outgoing unit wavevectors $\hat{\mathbf{k}}_i$ and $\hat{\mathbf{k}}_o$, we introduce two unit vectors $\hat{\mathbf{e}}_1 = \hat{\mathbf{k}}_i$ and $\hat{\mathbf{e}}_2 = \hat{\mathbf{k}}_i \times (\hat{\mathbf{k}}_i \times \hat{\mathbf{k}}_f)/|\hat{\mathbf{k}}_i \times (\hat{\mathbf{k}}_i \times \hat{\mathbf{k}}_f)|$, which constitute an orthonormal basis of the scattering plane. In the scattering plane, we may decompose the velocity $\mathbf{v}$ of the scatterer along $\hat{\mathbf{e}}_1$ and $\hat{\mathbf{e}}_2$ so that

$$\mathbf{v} = v_1\hat{\mathbf{e}}_1 + v_2\hat{\mathbf{e}}_2 \tag{9}$$

We know that v_1 is determined from the incident photon and we choose v_2 using a Gaussian random deviate. Then the velocity component $v_{\rm sc}$ along the propagation direction of the scattered radiation becomes

$$v_{\rm sc} = \mathbf{v}\cdot\hat{\mathbf{k}}_o = v_1\cos\theta + v_2\sin\theta, \tag{10}$$

where $\cos\theta = \hat{\mathbf{k}}_i\cdot\hat{\mathbf{k}}_o$. From this consideration, the old Doppler factor v_1 is renewed to become $v_{\rm sc}$.

We use an isotropic scattering phase function in this work for simplicity. In the case of resonance scattering, the scattering phase function differs according to the angular momentum quantum numbers of the two levels (e.g., Lee 1994). However, we are interested in emission nebulae with sufficiently large line center optical depths so that multiple scattering effectively results in isotropic angular distribution for scattered radiation.

Another uniform random number X' is generated and in case it is smaller than the branching ratio for deexcition to 2s then the new photon is still an Hα photon and otherwise we have a Lyβ photon (e.g., Chang et al. 2015). A given photon is traced until it escapes from the emission region keeping its identity and the Doppler factor along its propagation.

First, no consideration of transition into the ground state is made as a check of our Monte Carlo code. When only Hα treated as a resonance line, Figure 2 shows hypothetical profiles of Hα emergent from

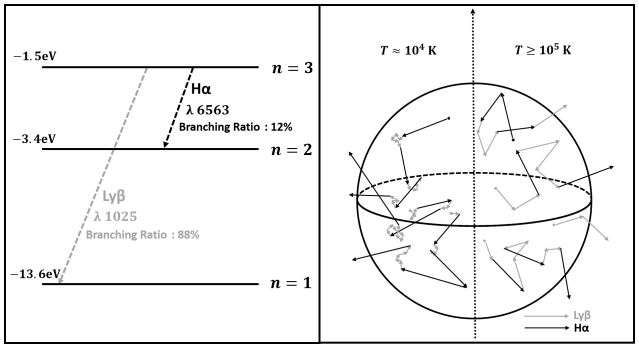

Figure 1. Schematic illustration of radiative transfer of Hα and Lyβ in an ionized nebula. The branching ratio into Lyβ transition from $3p$ is 0.88 and that into Hα is 0.12. As temperature goes up, the mean free path of Lyβ increases due to population shift to $2s$ from $1s$.

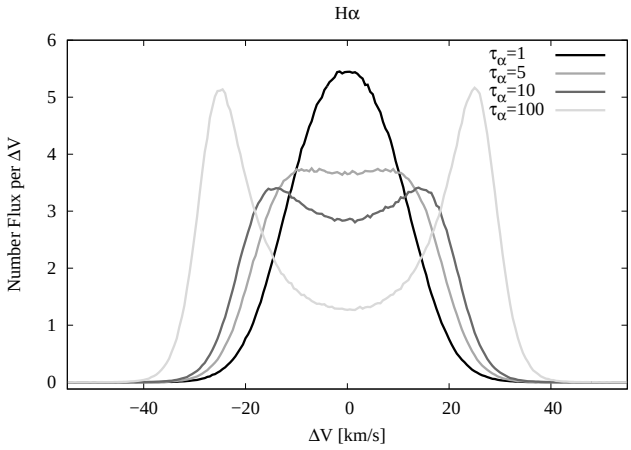

Figure 2. Line profiles of Hα emergent from a scattering medium for various values of line center optical depth τ ranging from 1 to 100. No consideration of transition into the ground state is made, treating Hα as a genuine resonance line.

a spherical medium. We collect all the photons escaping from the emission region according to their Doppler factor or wavelength. The temperature of the sphere is taken to be $T = 10^4$ K and line photons are generated with a Gaussian distribution. For $\tau_\alpha = 1$, the effect of diffusion is negligible and the emergent profile traces the Maxwell-Boltzmann distribution with the thermal speed $v_{th} = 13$ km s^{-1}. As τ increases, more and more line center photons diffuse into the wing regime before they make their escape from the medium resulting in clear double peak profiles. For $\tau_\alpha = 10$, 100 and 1000, the peaks are found to occur at $v = \pm 14$ km s^{-1} and 22 km s^{-1} respectively.

3. LINE TRANSFER OF Hα AND LYβ

In Figure 3, we show a representative result from our Monte Carlo calculation of Hα-Lyβ transfer. The spherical emission nebula is characterized by $\tau_\alpha = 10$ and $T = 3 \times 10^4$ K. The two top panels show line profiles of emergent Hα and Lyβ shown in Doppler factor space in units of km s^{-1}. The vertical axis shows the number flux density. The two bottom panels show the same result in wavelength space in units of Å. In this particular example, the ratio of the emergent number fluxes of Lyβ and Hα is 0.486.

We obtain symmetric double peak profiles for both Hα and Lyβ. In the Doppler factor space, the separation of the two peaks is 80 km s^{-1} for Hα and for Lyβ a slightly larger value of 105 km s^{-1} is obtained. We may also characterize the symmetric double peak profiles by the ratio of the number flux density values at the peaks and the center dip, which are found to be 1.4 and 2.9 for Hα and Lyβ, respectively.

3.1. Dependence on Line Center Optical Depth and Temperature

In Figure 4, we show line profiles of Hα and Lyβ by varying the line center optical depth τ_α for a fixed value of $T = 3 \times 10^4$ K. With this $T = 3 \times 10^4$ K it turns out that the ratio of optical depths $\tau_\beta/\tau_\alpha \sim 15$ so that these two transitions have comparable scattering optical depths. The vertical axis shows the number of emergent photons per unit Doppler factor in units of km s^{-1}.

As τ_α increases, photons initially in the core part diffuse out entering into the wing regime in frequency space, which results in line profile broadening. In the Doppler factor space, the Lyβ profile is always broader than that of Hα, which is expected from the fact that $\tau_\beta > \tau_\alpha$. The profiles of emergent Lyβ shown in this figure are doubly peaked through frequency diffusion. In contrast, Hα is singly peaked in the case of $\tau_\alpha = 1$ for which frequency diffusion is minimal. As $\tau_\alpha \geq 5$ the profile flattens and begins to develop a clear double peak structure. In this figure, the largest flux ratio ~ 1.03 of Lyβ to Hα is obtained in the case of the smallest scattering optical depth $\tau_\alpha = 1$ considered in this work.

Figure 5 shows various line profiles of emergent Hα and Lyβ from a spherical emission region with a fixed value of $\tau_\alpha = 10$. The temperature of the medium ranges from 10^4 K to 10^5 K. As is verified in the figure, almost no Lyβ is observed in the case $T = 10^4$ K, justifying the use of the case B recombination theory in a typical emission nebula. However, as T increases, the emergent Lyβ becomes strong and broad.

According to Osterbrock (1962), the mean scattering number of resonance line photons before escape is linearly proportional to the line center optical depth. This implies that the escape probability is inversely related to the line center optical depth, which, in turn, leads to the relation that the emergent line flux is also inversely proportional to the line center optical depth. Because the ratio of the line center optical depths of Lyβ and Hα is directly related to the ratio of the $1s$ and $2s$ populations, the ratio of emergent number flux is mainly determined by the Boltzmann factor or equivalently the temperature of the medium.

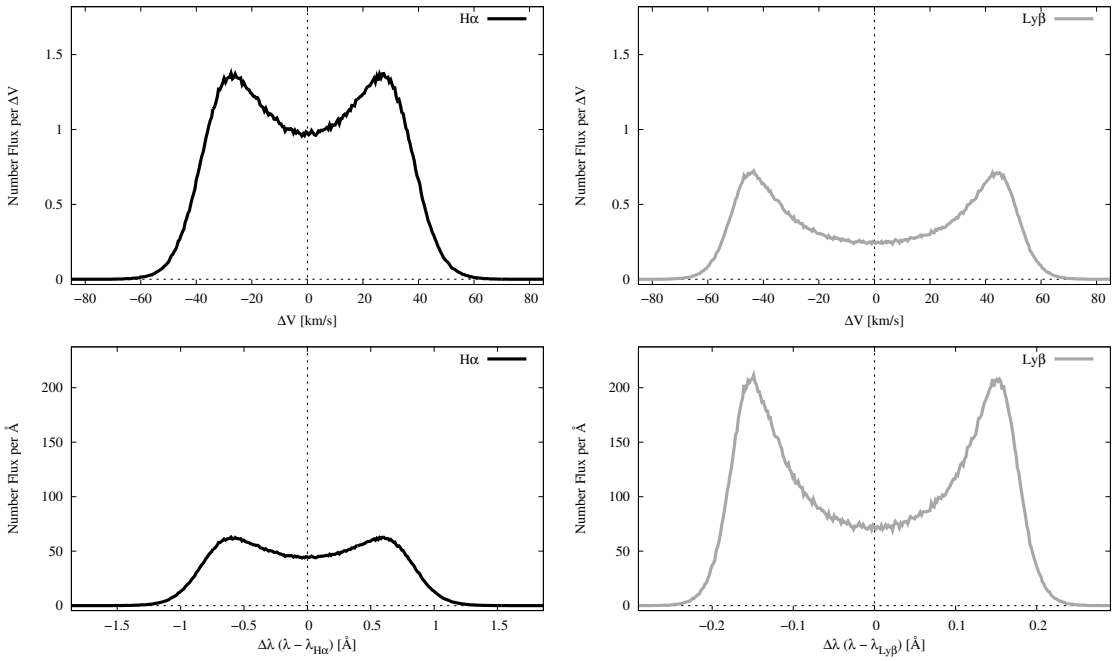

Figure 3. Representative line profiles of emergent Hα and Lyβ shown in Doppler factor space (top panels) and wavelength space (bottom panels). The emission nebula is characterized by the Hα line center optical depth $\tau_\alpha = 10$ and temperature $T = 3 \times 10^4$ K. It is noted that Lyβ exhibits wider profiles in Doppler space than Hα.

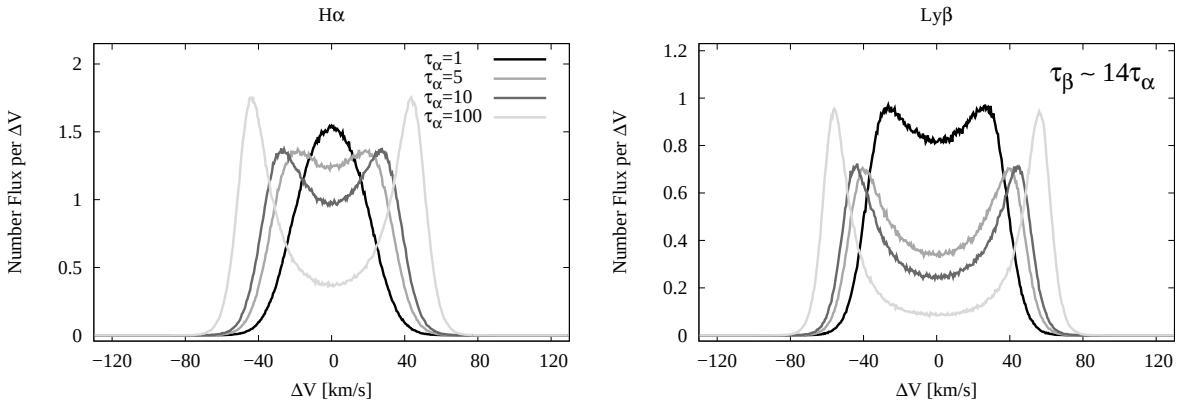

Figure 4. Line profiles of Hα (left) and Lyβ (right) for various values of Hα line center optical depth τ_α. Here, the nebular temperature is fixed $T = 3 \times 10^4$ K.

3.2. Flux Ratios in $(\tau - T)$ Space

In Figure 6, we present a suite of line profiles of Hα and Lyβ emergent from a spherical emission nebula with a uniform density. From left to right panels we increase the line center optical depth τ_α of Hα and from top to bottom panels the medium temperature increases from $T = 10^4$ K to $T = 10^5$ K. The top-left panel for a small optical depth with $T = 10^4$ K, the emergent profile of Hα is very close to the Gaussian function corresponding to the Maxwell-Boltzmann distribution with the same temperature. The profiles shown by a solid black line are the result that would be obtained if there is no Lyβ scattering channel. Profiles of Hα and Lyβ are shown by bright gray and dark gray solid lines, respectively.

For $T = 10^4$ K, Lyβ is almost negligible, so that Hα behaves effectively like a resonance line. This justifies use of the case B recombination theory, where no higher Lyman series lines than Lyα are emergent with measurable fluxes. For $T = 2 \times 10^4$ K a sizable fraction amounting ~ 10 percent of emergent line photons are Lyβ. It is also interesting to note that Lyβ exhibits double peak profiles for $T = 2 \times 10^4, 3 \times 10^4$ K and $\tau_\alpha = 1$, for which Hα profiles are singly peaked.

In Figure 7, we present a color map of the ratio of the number fluxes of Hα and Lyβ in the (τ_α, T) space. The contours are connecting those points of (τ_α, T) yielding the same values of the number flux ratio. The overall tendency is that Lyβ flux becomes relatively stronger as T increases and τ_α decreases. It is readily seen that a negligible flux of Lyβ is obtained

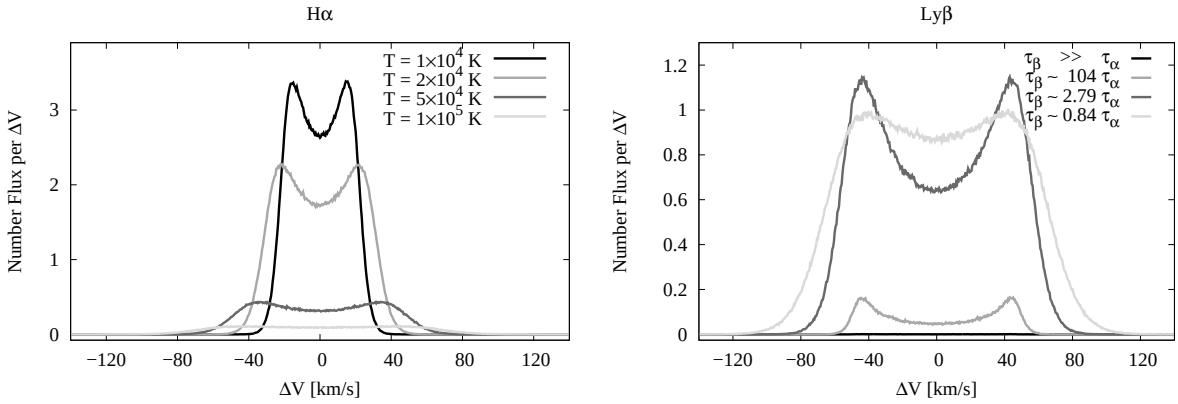

Figure 5. Line profiles of Hα (left) and Lyβ (right) for various values of T. Here, the Hα line center optical depth is fixed to $\tau_\alpha = 10$.

in the case $T \sim 10^4$ K. However, for $T = 2 \times 10^4$K a considerably large ratio of the number fluxes amounting to ~ 0.1 is obtained. When the medium temperature $T \geq 3 \times 10^4$ K the number flux ratio exceeds 0.5, which is quite significant.

3.3. Profile Widths of Hα and Lyβ

Osterbrock (1962) argued that the profile width of Lyα emerging from a medium with high scattering optical depth τ is approximately proportional to $\sqrt{\ln \tau}$. This expression results from the assumption that resonance line photons escape after attaining frequency shift so that the medium eventually becomes optically thin. Introducing a frequency parameter $x = (\nu - \nu_0)/\nu_{th}$ in units of the Doppler frequency width $\nu_{th} = \frac{v_{th}}{c}\nu_0$ with ν_0 being line center frequency, the escape frequency x_1 will satisfy

$$\tau_\alpha e^{-x_1^2} \simeq 1, \tag{11}$$

leading to the dependence on $\sqrt{\ln \tau_\alpha}$.

We quantify the diffusion process in frequency space by estimating the half width at half maximum (HWHM) of line profiles. In the right panel of Figure 8, we show the method to measure the HWHM and the result of our Monte Carlo calculation. Given τ_α we consider 31 cases of T in the range 10^{4-5} K to obtain emergent Hα profiles. The HWHM of Hα is divided by v_{th} in order to clarify the diffusive nature of line radiative transfer in frequency space. The average and the standard deviation of the HWHM are subsequently obtained to be shown in the right panel by circles with an error bar. The smallness of the error bars justifies this approach to present the profile width as a function τ_α.

The data can be fit with a function $f(\tau_\alpha)$

$$f(\tau_\alpha) = 0.91\sqrt{\ln \tau_\alpha} + 0.38. \tag{12}$$

A good fit is obtained for $\tau_\alpha > 3$, where Equation (11) is approximately valid. However, for $\tau_\alpha < 3$, the optical depth is not high enough to make the radiative transfer diffusive in frequency space. This is also confirmed from the single peak profiles exhibited by Hα in this low optical depth regime.

Figure 9 presents the HWHM of Lyβ and Hα profiles in units of v_{th} in the 2 dimensional parameter space of τ_α and T. In the case of Hα, the HWHM appears to depend only on line center optical depth τ_α and is almost independent of T. This is attributed to normalization by v_{th}, which corresponds to the one-step interval as we approximate a diffusion phenomenon by a random walk process. Lyβ profile widths are very noisy for $T \sim 10^4$ because of the small number statistics of escaping Lyβ. According to Equation (6), the Lyβ optical depth τ_β is larger than the Hα counterpart τ_α, which gives rise to broader Lyβ than Hα.

3.4. Scattering Numbers of Hα and Lyβ

In Figure 10, we show the scattering numbers of Lyβ and Hα before escape for various τ_α and the temperature of the emission region. For comparison in the third panel we show the scattering number of Hα treating it as a resonance line by setting the branching ratio into Lyβ to be null. In the case of resonance line radiative transfer, the scattering number is approximately proportional to the line center optical depth (e.g., Adams 1972).

In the second panel, the scattering number of Hα is slightly larger than that expected for resonance line photons in a medium with the same line center optical depth, which is attributed to an additional contribution from the Lyβ scattering channel. The contribution of the Lyβ channel increases as the level $n = 1$ population increases. This implies that given τ_α the scattering number of emergent Hα decreases as T increases.

In the first panel, the Monte Carlo data for $T \sim 10^4$ K are noisy, which is attributed to a very weak emergent Lyβ flux in these cases. Furthermore, the scattering number is rather small compared to the line center optical depth. This is explained by the fact that the weak emergent Lyβ flux is significantly contributed by those line photons originating near the boundary. It is also noteworthy that as $T \geq 3 \times 10^4$ K the scattering numbers of Lyβ and Hα become comparable to each other.

It should be noted that the left and center pan-

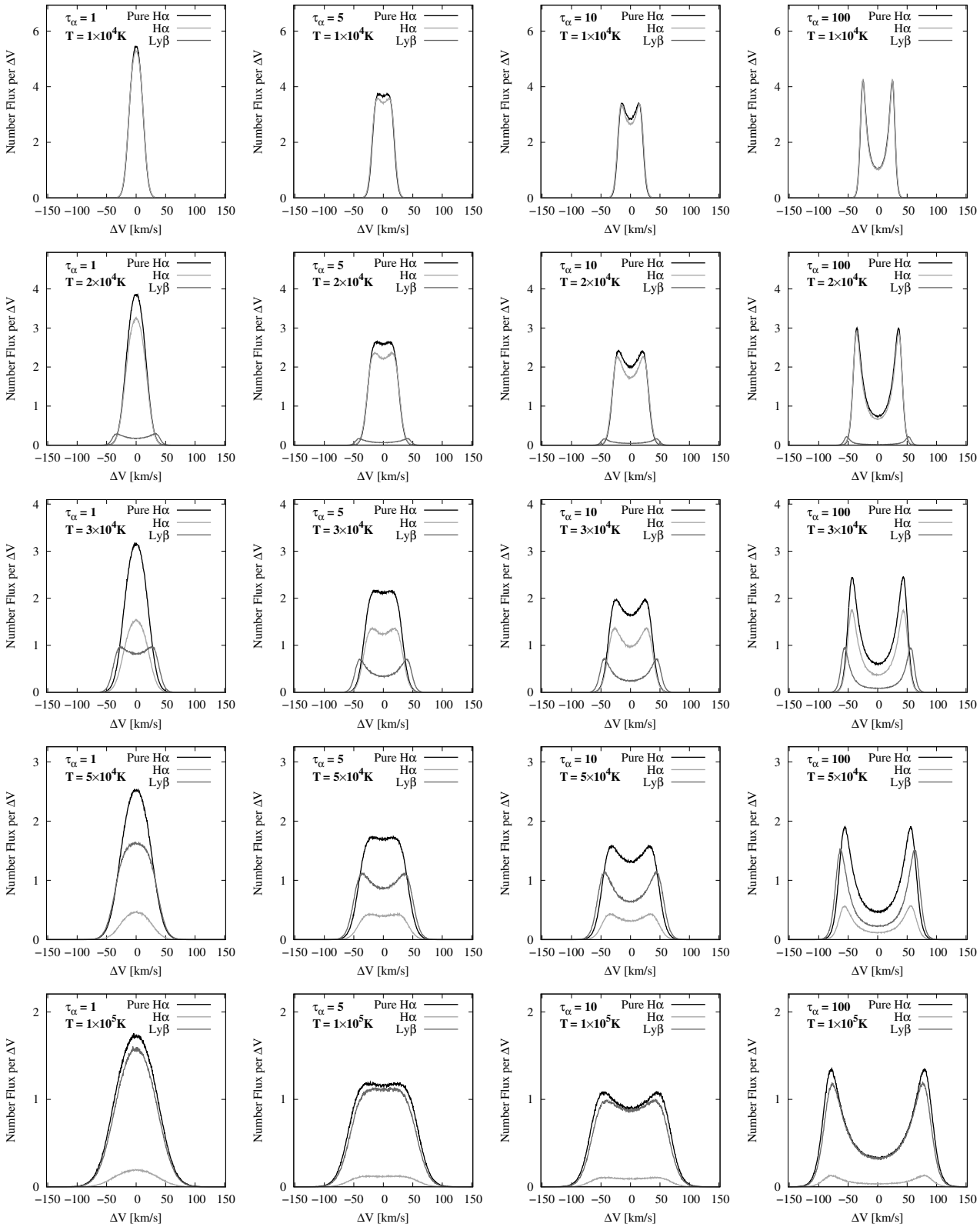

Figure 6. Line profiles and number fluxes of emergent Hα and Lyβ for various Hα line center optical depth τ_α and temperature T. The ranges of T and τ_α considered in this work are 10^4 K $\leq T \leq 10^5$K and $1 \leq \tau_\alpha \leq 100$. The black curve is the emergent profile of Hα with no consideration of branching into Lyβ transition. Bright gray and dark gray lines show the profiles of Hα and Lyβ, respectively.

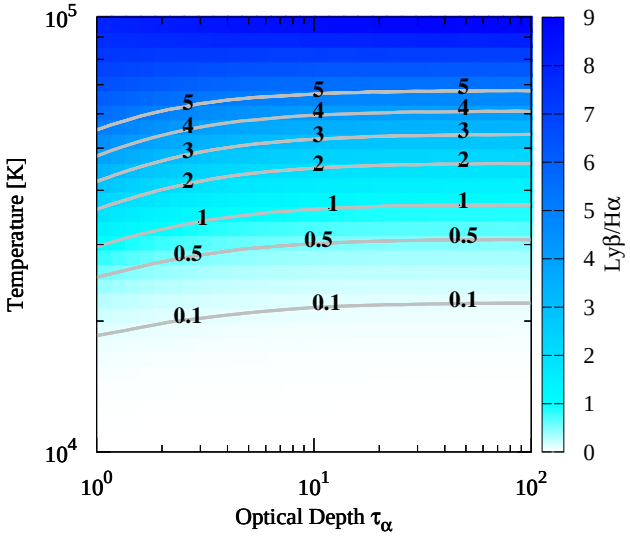

Figure 7. Two dimensional plot of the number flux ratios of emergent Hα and Lyβ for various values of Hα line center optical depth τ_α and temperature T. As is discussed in the text, more Lyβ photons escape as T increases and τ_α decreases.

els show remarkably similar behavior of the scattering number. If τ_α and τ_β are both large, then the transfer processes of Ly beta and H alpha are virtually same and the final scattering determines the identity of the escaping photon. Therefore as far as τ_α is larger than unity, we expect the virtually similar dependence of scattering number of H alpha and Ly beta on tau and temperature.

4. APPLICATION TO BROAD Hα WINGS IN SYMBIOTIC STARS

Spectroscopic observations of symbiotic stars reveal that Hα emission lines exhibit broad wings that may extend to 10^3 km s^{-1} (e.g., Van Winckel et al. 1993; Ivison et al. 1994). Such broad wings of Hα are also found in planetary nebulae including M2-9 (Balick 1989) and IC 4997 (Lee & Hyung 2000). Van de Steene et al. (2000) reported that broad Hα wings are found in post AGB stars. It appears that many active galactic nuclei also exhibit very broad Hα wings in their spectra.

Broad Hα wings can be formed in a hot tenuous wind (e.g., Skopal 2006). Many symbiotic stars and planetary nebulae show P Cygni type profiles in far UV resonance lines including O VI$\lambda\lambda$1032 and 1038 and C IV$\lambda\lambda$1548 and 1551, indicative of the fast outflows from the center. About 10 percent of quasars show broad absorption trough in their emission lines, which are presumably formed through resonance scattering in fast outflows from the central supermassive black holes.

Broad Hα wings can also be formed through scattering of Hα photons with free electrons. Sekeras & Skopal (2012) proposed that broad wings around O VI$\lambda\lambda$1032, 1038 in symbiotic stars can be well fitted from Thomson scattering in a medium with Thomson optical depth $\tau_{Th} \sim 0.05-0.8$ and electron temperature $T_e \sim 1.5\times10^4$ K $- 4\times10^4$ K (see also Schmid et al. 1999).

An interesting astrophysical mechanism giving rise to broad Hα wings can be obtained through Raman scattering of Lyβ with atomic hydrogen. Here, the term 'Raman scattering' refers to inelastic scattering of a far UV photon incident upon a hydrogen atom in the ground state, which finally de-excites into $2s$ state with a reemission of an optical photon. A line photon of O VIλ 1032 is Raman scattered to become an optical photon with $\lambda = 6825$ Å (Schmid 1989) and a far UV photon near Lyβ is Raman scattered to appear near Hα. The wavelengths of the incident photon and its Raman scattered one, λ_i and λ_o are related by

$$\lambda_o^{-1} = \lambda_i^{-1} - \lambda_\alpha^{-1} \quad (13)$$

where λ_α is the wavelength of Lyα. The inelasticity of scattering results in significant profile broadening by a factor of λ_o/λ_i, which is about 6 in the case of Lyβ-Hα scattering. The operation of Raman scattering to form Hα wings requires a sizable number of Lyβ photons from an emission nebula that subsequently enter a neutral region

In Figure 11, we show a schematic illustration for formation of Hα wings through Raman scattering of Lyβ. In this geometry, the Lyβ-Hα emission region is surrounded by a neutral hemispheric region, where Raman scattering of Lyβ takes place. The Lyβ-Hα emission source located at the center is the same as the emission nebula illustrated in the right panel of Figure 1. The temperature and the optical depth of the emission source are taken to be $T = 5\times10^4$ K and $\tau_\alpha = 1$, respectively. The hemispheric neutral region is characterized by the column density $N_{HI} = 10^{19}$ cm^{-2}. The bottom three panels in Figure 11 show resultant wing profiles. It is noticeable that the HWHM of Hα wings in the bottom left panel is 125 km s^{-1} broader than the HWHM of Lyβ directly emergent from the source.

In Figure 12, we present the line profiles of Hα core and wing parts, formed in the environment described in Figure 11. We consider two values of the temperature of Lyβ-Hα emission region $T = 3\times10^4$ K and 5×10^4 K. We also vary the optical depth $\tau_\alpha = 1-100$, and the column density $N_{HI} = 10^{19-20}$ cm^{-2}. In the case of $N_{HI} = 10^{19}$ cm^{-2}, single broad wing profiles are obtained. However, as we increase $N_{HI} = 10^{20}$ cm^{-2} and $\tau_\alpha > 5$, the wing profiles tend to exhibit broad double peak. For example, the peak separation of broad Hα wings is 530 km s^{-1} with $\tau_\alpha = 10$, $T = 5\times10^4$ K and $N_{HI} = 10^{20}$ cm^{-2}. However, if there is any bulk motion > 30 km s^{-1} in the Lyβ-Hα emission region, the emergent profiles convolved with the bulk motion may appear as single broad wings.

Arrieta & Torres-Peimbert (2003) showed that the wing profiles are excellently fitted using a function $(\lambda - \lambda_{H\alpha})^{-2}$, which is consistent with Raman scattering cross section around Lyβ (e.g., Lee 2000; Nussbaumer et al. 1989; Schmid 1989). In this section, we present

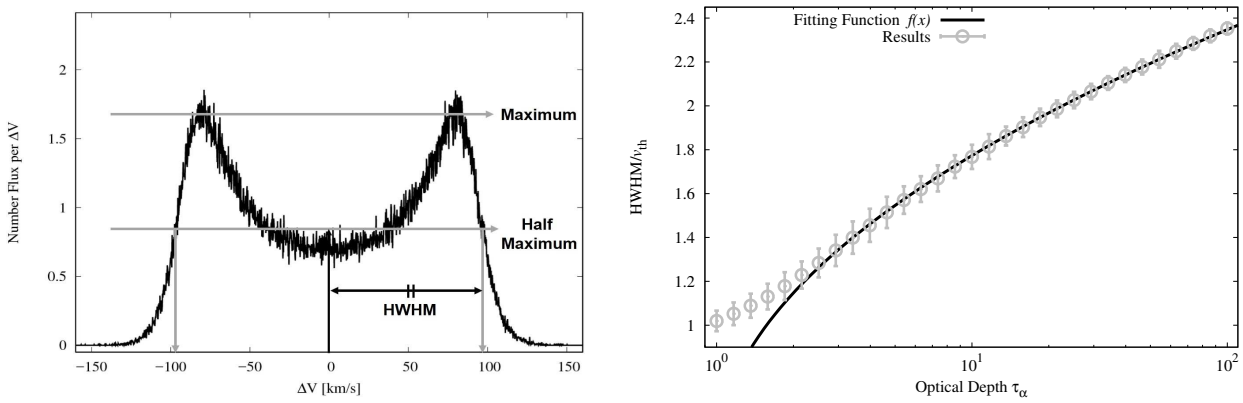

Figure 8. Profile width as a function of Hα line center optical depth. The left panel illustrates the definition of the half width at half maximum (HWHM). The right panel shows HWMH of Hα divided by the thermal speed v_{th}. We obtain the HWHM by averaging the Monte Carlo data obtained for 31 values of T in the range of $10^4 - 10^5$ K for a given value of τ_α. The error bars represent one standard deviation. The fitting function $f(\tau_\alpha)$ is also shown by a solid curve, where $f(\tau_\alpha) = 0.91(\ln \tau_\alpha)^{1/2} + 0.38$.

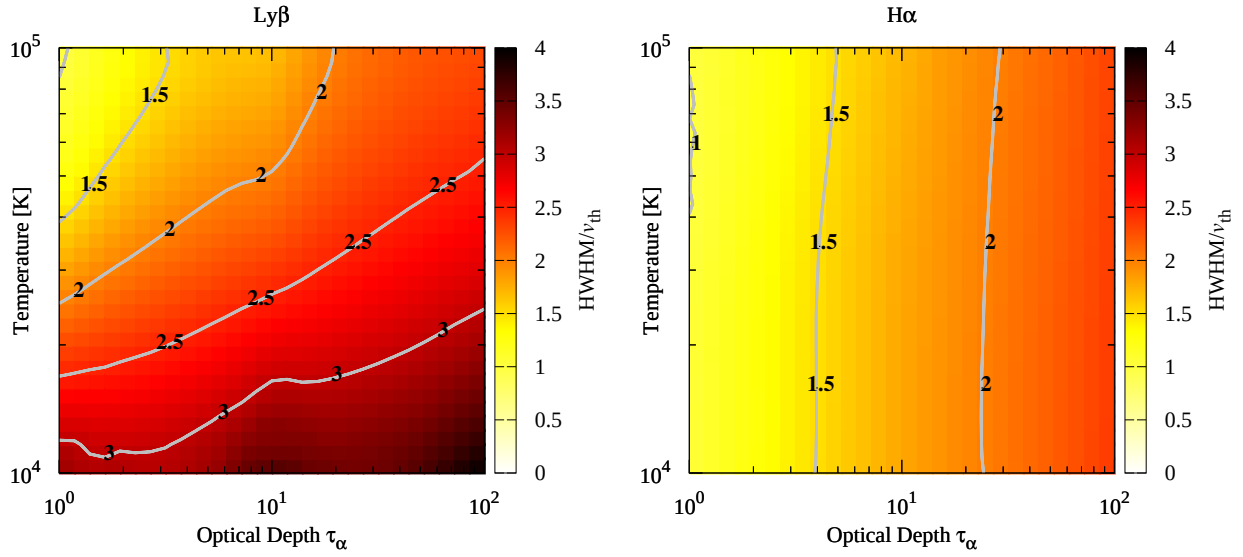

Figure 9. Profile widths of Lyβ (left panel) and Hα (right panel) normalized by the thermal velocity v_{th} for various values of τ_α and T of the emission region. The horizontal axis is line center optical depth τ_α and the vertical axis is the temperature T of the emission nebula.

the parameter space consisting of τ_α and T in which Lyβ is emergent sufficiently to account for Hα wings typically observed in symbiotic stars.

5. SUMMARY AND DISCUSSION

In this work we have used a Monte Carlo code to treat the radiative transfer of Lyβ-Hα line photons in an optically thick spherical emission region. When the electron temperature of the emission region is lower than 20 000 K, escape of Lyβ is quite insignificant due to small population of hydrogen atoms in $n = 2$ levels. However, it is found that for temperatures $\geq 3\times10^4$ K the emergent Lyβ flux becomes comparable to that of Hα playing an important role as a coolant of the emission region. As the line center optical depth of Hα increases, the emergent line profile of Hα becomes broader.

Symbiotic stars are known to exhibit strong Hα emission with broad wings and absorption trough blueward of its line center. Raman scattering of Lyβ by atomic hydrogen results in profile broadening by a factor $6563/1025 = 6.4$, leading to formation of broad wings around Hα. The current work lends strong support to the proposal that broad Hα wings found in many symbiotic stars have their origin in Raman scattering of Lyβ emergent in the Hα thick emission nebula around the white dwarf.

The $2s$ level population can be significantly enhanced due to Raman scattering of far UV radiation.

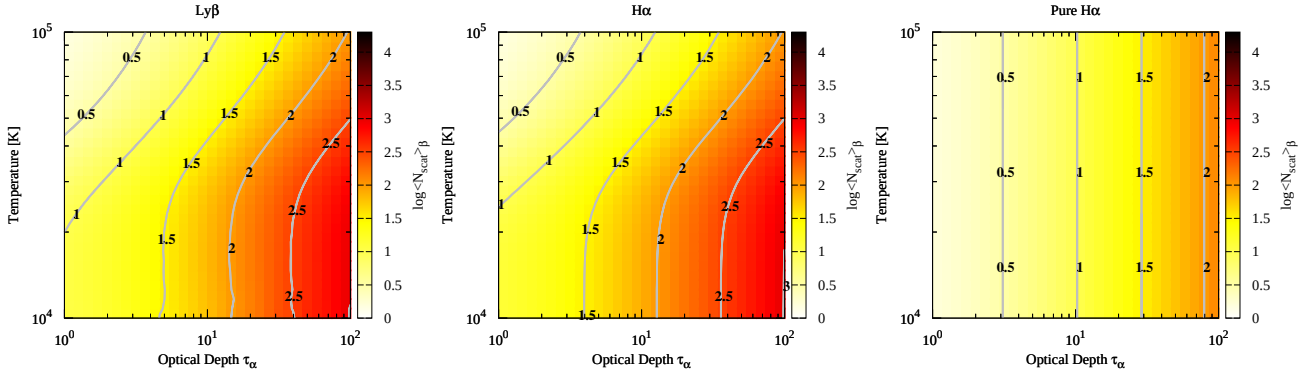

Figure 10. Scattering numbers of Hα and Lyβ before escape for various τ_α and the temperature of the emission region. The horizontal axis is line center optical depth and the vertical axis is the temperature of the emission nebula.

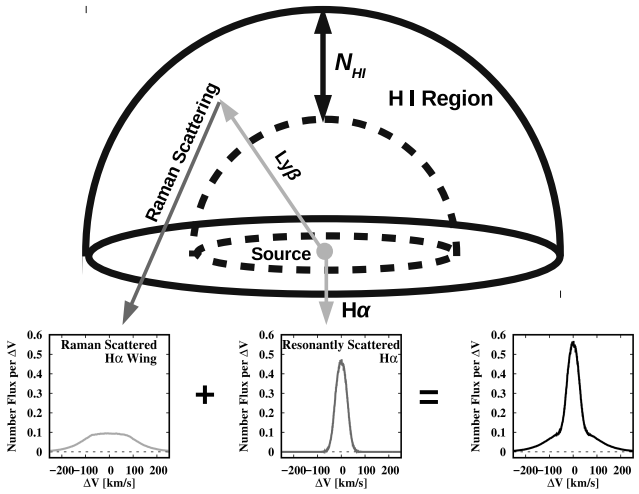

Figure 11. Schematic illustration of forming Hα wings in a hemispheric neutral region surrounding a central H II region through Raman scattering of Lyβ. The center emission source is a spherical ionized region shown in the right panel of Figure 1. N_{HI} is the H I column density of hemispheric neutral region. The center panel shows Hα emission profile emergent from the source characterized with $T = 5 \times 10^4$K and $\tau_\alpha = 1$. The left panel shows Raman scattering wings obtained with $N_{HI} = 10^{19}\mathrm{cm}^{-2}$ The right panel shows the composite profile of Hα emission and wings.

This is because $2s$ level is mainly depopulated by continuum two-photon decay, which is characterized by the decay time of about 8 seconds. In particular, strong O VI resonance doublet lines are incident on H I region to be Raman scattered leaving the H atom in the $2s$ state (e.g. Heo et al. 2015). This effect may be important in the blueward dip of Hα profiles observed in many symbiotic stars.

This work is also expected to shed some light on the interpretation of the Balmer decrement that deviates from the case B recombination theory in symbiotic stars (e.g., Schwank 1997). In particular, the case B recombination dictates the flux ratio of $F_{H\alpha}/F_{H\beta} = 2.86$, and many symbiotic stars exhibit stronger Hα than this generic value. Escape of higher Lyman series photons will produce complicated flux ratios of Balmer fluxes deviating from the case B theory.

In an Hα thick medium, escape in the form of Lyβ may reduce the Hα flux from the case B value. However, the medium is expected to be also optically thick to Hβ, escape of Hβ can be achieved by changing its identity as Paα. This implies that a nebula with significant $2s$ population is expected to exhibit $F_{H\alpha}/F_{H\beta}$ ratio different than the case B value of 2.86. A more refined radiative transfer study incorporating Paschen and higher Lyman and Balmer transitions is required to provide a more satisfactory answer.

Hydrogen emission lines are an important tool to study the cosmic star formation history and Lyα is particularly useful to probe the galactic environment associated with star formation activities in the early universe with z higher than 2. Being a prototypical resonance line, Lyα photons suffer enormously large number of scatterings before escape leading to formation of characteristic P Cygni profiles or profiles suppressed in the blue part (e.g., Ahn et al. 2003; Dijkstra 2014). Recent studies show that many Lyman alpha emitters are surrounded by a neutral halo, where Lyα photons appear to be resonantly scattered.

One good example of Lyβ emission can be found in quasars, where Lyβ and O VI form a broad composite emission line. Laor et al. (1994, 1995) have analyzed UV spectra of quasars with redshifts in the range $0.165 \leq z \leq 2.06$ to investigate the properties of emission lines including Lyα 1215+N V 1240 and Lyβ 1025+ O VI 1034. They deconvolved the composite broad emission lines to find the flux ratios of Lyβ/O VI $= 0.34 \pm 0.26$ and Lyβ/Lyα $= 0.059 \pm 0.04$. Vanden Berk et al. (2001) carried out similar analyses using spectra of quasars in an extended range of redshift $0.044 \leq z \leq 4.789$ from the *Sloan Digital Sky Survey*. The flux ratios found in their study are (Lyβ+O VI)/Lyα $= 0.096$ and Hα/Lyα $= 0.31$.

Cabot et al. (2016) investigated Lyα, C IV, and He II emission lines in Lyman α blobs, pointing out the presence of emission nebulae with temperature $\sim 2\times10^4$

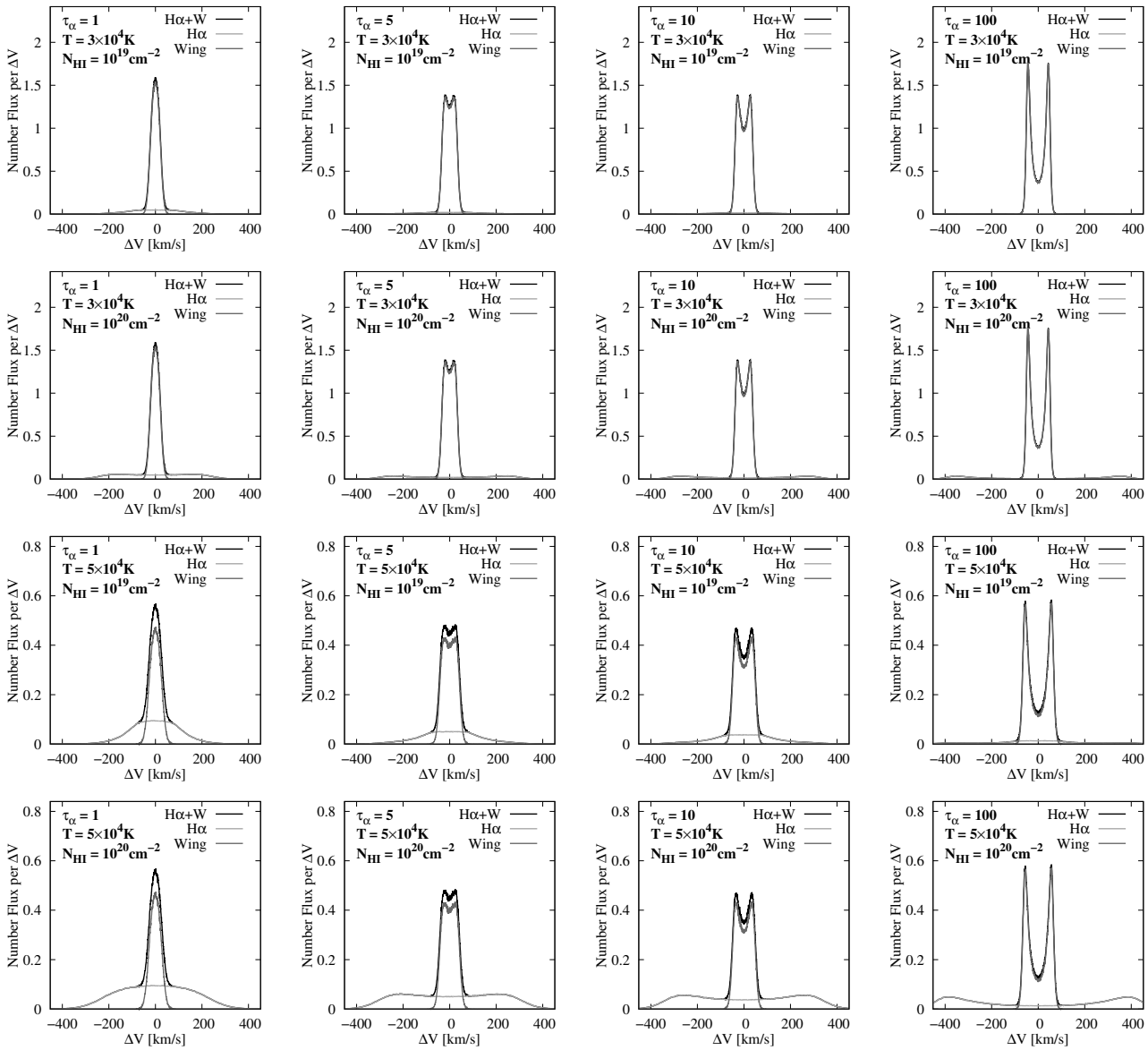

Figure 12. Line profiles and number fluxes of Raman scattered Hα wings (dark gray) and Hα emission (bright gray) in the model illustrated in Figure 11. The black solid lines show the total profiles combining the wings and emission. The source temperature $T = 3 \times 10^4$ K for the top two panels and $T = 5 \times 10^4$ K for the bottom two panels. The optical depth τ_α considered is in the range $1 \leq \tau_\alpha \leq 100$. Two values of $N_{HI} = 10^{19}$ cm^{-2} and 10^{20} cm^{-2} are considered.

for Lyα and $\sim 10^5$ K for C IV and He II. In this environment, Lyβ photons also escape from the hot nebular region and may suffer Raman scattering with hydrogen atoms that may reside possibly in the neighboring neutral halo. In this case we may predict that Hα will be characterized by very broad wings that may exceed the kinematic speed associated with the circumgalactic medium. IR spectroscopy using a space telescope such as *James Webb Space Telescope* can be performed to detect the broad wings around Balmer emission lines.

ACKNOWLEDGMENTS

We are very grateful to an anonymous referee for the constructive comments, which improved the presentation of the current paper. This research was supported by the Korea Astronomy and Space Science Institute under the R&D program (Project No. 2018-1-860-00) supervised by the Ministry of Science and ICT. The Monte Carlo calculation was performed by using the PC-cluster Polaris in KASI. Seok-Jun Chang is also particularly grateful to Dr. Jongsoo Kim for his help to parallize and improve the code in a much more efficient way.

REFERENCES

Adams, T. F. 1972, The Escape of Resonance-Line Radiation from Extremely Opaque Media, ApJ, 174, 439

Ahn, S.-H., Lee, H.-W., & Lee, H. M. 2003, P Cygni Type Lyα from Starburst Galaxies, MNRAS, 340, 863

Ahn, S.-H., Lee, & H.-W. 2015, Polarization of Lyman α

Emergent from a Thick Slab of Neutral Hydrogen, JKAS, 48, 195
Arrieta, A., & Torres-Peimbert, S. 2003, Broad Hα Wings in Nebulae around Evolved Stars and in Young Planetary Nebulae, ApJS, 147, 97
Balick, B. 1989, M2-9 - A Planetary Nebula with an Eruptive Nucleus?, AJ, 97, 476
Cabot, S. H. C., Cen, R., & Zheng, Z.2016, C IV and He II Line Emission of Lyman α Blobs: Powered by Shock-Heated Gas, MNRAS, 462, 1076
Chang, S.-J., Heo, J.-E., Di Mille, F., Angeloni, R., Palma, T., & Lee, H.-W. 2015, Formation of Raman Scattering Wings around H alpha, H beta, and Pa alpha in Active Galactic Nuclei, ApJ, 814, 98
Dijkstra, M. 2014, Lyα Emitting Galaxies as a Probe of Reionisation, PASA, 31, 40
Gnat, O., & Sternberg, A. 2007, Time-Dependent Ionization in Radiatively Cooling Gas, ApJS, 168, 213
Gronke, M., Dijkstra, M., McCourt, M., & Oh, S. P. 2016, From Mirrors to Windows: Lyman-Alpha Radiative Transfer in a Very Clumpy Medium, ApJL, 833L, 26
Godon, P., Sion, E. M., Levay, K., Linnell, A. P., & Szkody, P. 2012, An Online Catalog of Cataclysmic Variable Spectra from the Far-Ultraviolet Spectroscopic Explorer, ApJS, 203, 29G
Heo, J.-E., & Lee, H.-W. 2015, Accretion Flow and Disparate Profiles of Raman Scattered O VI $\lambda\lambda$1032, 1038 in the Symbiotic Star V1016 Cygni, JKAS, 48, 105
Ivison, R. J., Bode, M. F., & Meaburn, J. 1994, An Atlas of High Resolution Line Profiles of Symbiotic Stars. II. Echelle Spectroscopy of Northern Sky Objects, A&AS, 103, 201
Kenyon, S. 1986, The Symbiotic Stars (New York: Cambridge University Press)
Laor, A., Bahcall, J. N., Jannuzi, B. T., Schneider, D. P., & Green, R. F. 1995, The Ultraviolet Emission Properties of 13 Quasars, ApJS, 99, 1
Laor, A., Bahcall, J. N., Jannuzi, B. T., Schneider, D. P., Green, R. F., & Hartig, G. F. 1994, The Ultraviolet Emission Properties of Five Low-Redshift Active Galactic Nuclei at High Signal-To-Noise Ratio and Spectral Resolution, ApJ, 420, 110
Lee, H.-W. 1994, On the Polarization of Resonantly Scattered Emission Lines – Part Two – Polarized Emission from Anisotropically Expanding Clouds, MNRAS, 268, 49
Lee, H.-W. 2000, Raman-Scattering Wings of Hα in Symbiotic Stars, ApJL, 541, 25
Lee, H.-W. 2013, Asymmetric Absorption Profiles of Lyα and Lyβ in Damped Lyα Systems, ApJ, 772, 123
Lee, H.-W., & Hyung, S. 2000, Broad Hα Wing Formation in the Planetary Nebula IC 4997, ApJL, 530, 49
Netzer, H. 2015, Revisiting the Unified Model of Active Galactic Nuclei, ARA&A, 53, 365
Neufeld, D. A. 1990, The Transfer of Resonance-Line Radiation in Static Astrophysical Media, ApJ, 350, 216
Nussbaumer, H., Schmid, H. M., & Vogel, M. 1989, Raman Scattering as a Diagnostic Possibility in Astrophysics, A&A, 211, 27
Nuñez, N. E., Nelson, T., Mukai, K., Sokoloski, J. L., & Luna, G. J. M. 2016, Symbiotic Stars in X-Rays. III. Suzaku Observations, ApJ, 824, 23
Osterbrock, D. E. 1962, The Escape of Resonance-Line Radiation from an Optically Thick Nebula, ApJ, 135, 195
Ouchi, M., Shimasaku, K., Furusawa, H., Saito, T., & Yoshida, M. 2010, Statistics of 207 Lyα Emitters at a Redshift Near 7: Constraints on Reionization and Galaxy Formation Models, ApJ, 723, 869
Rybicki, G. B., & Lightman, A. P. 1985, Radiative Processes in Astrophysics (New York: John Wiley & Sons)
Saslow W. M., & Mills D. L. 1969, Raman Scattering by Hydrogenic Systems, Phys. Rev., 187, 1025
Sakurai J. J. 1967, Advanced Quantum Mechanics (Boston: Addison-Wesley)
Schmid, H. 1989, Dentification of the Emission Bands at 6830, 7088A, A&A, 211, 31
Schmid, H. et al. 1999, ORFEUS Spectroscopy of the O BT VI Lines in Symbiotic Stars and the Raman Scattering Process, A&A, 348, 950
Schwank, M., Schmutz, W., & Nussbaumer, H. 1997, Irradiated Red Giant Atmospheres in S-Type Symbiotic Stars, A&A, 319, 166
Sekeras, M., & Skopal, A. 2012, Electron Optical Depths and Temperatures of Symbiotic Nebulae from Thomson Scattering, MNRAS, 427, 979
Sion, E. M., Godon, P., Mikolajewska, J., Sabra, B., & Kolobow, C. 2017, FUSE Spectroscopy of the Accreting Hot Components in Symbiotic Variables, AJ, 153, 160
Skopal, A. 2005, Disentangling the Composite Continuum of Symbiotic Binaries. I. S-Type Systems, A&A, 440, 995
Skopal, A. 2006, Broad Hα Wings from the Optically Thin Stellar Wind of the Hot Components in Symbiotic Binaries, A&A, 457, 1003
van de Steene, G. C., Wood, P. R., & van Hoof, P. A. M. 2000, Hα Emission Line Profiles of Selected Post-AGB Stars, ASPC, 199, 191
Vanden Berk, D. E., et al. 2001, Composite Quasar Spectra from the Sloan Digital Sky Survey, AJ, 122, 549
Van Winckel, H., Duerbeck, H. W., & Schwarz, H. E. 1993, An Atlas of High Resolution Line Profiles of Symbiotic Stars - Part One - Coud Echelle Spectrometry of Southern Objects and a Classification System of Hα Line Profile, A&AS, 102, 401
Yang, Y., Zabludoff, A., Jahnke, K., Eisenstein, D., & Dav, R. 2011, Gas Kinematics in Lyα Nebulae, ApJ, 735, 87